



## ISTITUTO NAZIONALE DI RICERCA METROLOGICA Repository Istituzionale

Towards a sustainable approach for sound absorption assessment of building materials:  
Validation of small-scale reverberation room measurements

This is the author's accepted version of the contribution published as:

*Original*

Towards a sustainable approach for sound absorption assessment of building materials: Validation of small-scale reverberation room measurements / Shtrepi, Louena; Prato, Andrea. - In: APPLIED ACOUSTICS. - ISSN 0003-682X. - 165:(2020), p. 107304. [10.1016/j.apacoust.2020.107304]

*Availability:*

This version is available at: 11696/75674 since: 2023-06-15T13:30:53Z

*Publisher:*

ELSEVIER SCI LTD

*Published*

DOI:10.1016/j.apacoust.2020.107304

*Terms of use:*

This article is made available under terms and conditions as specified in the corresponding bibliographic description in the repository

*Publisher copyright*

(Article begins on next page)

1 **Towards a sustainable approach for sound absorption assessment of building materials:**  
2 **validation of small-scale reverberation room measurements** <sup>a)</sup>

3

4 Authors: Louena Shtrepi<sup>1</sup>, Andrea Prato<sup>2</sup>

5 <sup>1</sup>Politecnico di Torino, Torino, Italy

6 <sup>2</sup>INRiM - Istituto Nazionale della Ricerca Metrologica, Torino, Italy

7

8 e-mail addresses: louena.shtrepi@polito.it, a.prato@inrim.it

9

10 Corresponding author: Louena Shtrepi

11 E-mail address: louena.shtrepi@polito.it

12 Postal address: Department of Energy (DENERG), Corso Duca degli Abruzzi 24, 10129, Torino,

13 Italy

---

<sup>a)</sup> Part of this work was presented in Proceedings of the 23rd International Congress on Acoustics, 2019, Aachen, Germany

14 **Abstract**

15

16 The research and development phase of sound absorptive building materials by designers, engineers,  
17 acoustic consultants and architects need tools for fast, inexpensive preliminary comparison tests on  
18 products or acoustic systems. The existing methods exhibit some drawbacks: the impedance tube (IT)  
19 is not suitable for 3D systems, while the full-scale reverberation room (FSRR) requires test samples  
20 of large dimensions. To overcome these limitations, this work aims to explore the capabilities of  
21 small-scale reverberation rooms (SSRR) of about 3 m<sup>3</sup> located at Politecnico di Torino in evaluating  
22 the random-incidence sound absorption coefficient. In order to define the range of application and  
23 reliability of the method, the considered factors are the sample area and its orientation on the room  
24 floor. Four different materials have been tested by applying IT, FSRR and SSRR. The absorption  
25 coefficients data obtained with SSRR are compatible with the FSRR benchmarking in the 400-5000  
26 Hz frequency range for three porous materials, and in the range 1000-5000 Hz for the thin rigid  
27 material. Therefore, the SSRR can be considered as a reliable alternative for the sound absorption  
28 characterization in these ranges for this kind of materials, leading to several benefits. Among them,  
29 samples with reduced size can be evaluated with a cheaper equipment in a short time, increasing the  
30 overall economical sustainability of the measurement process; in turn, this can encourage designers  
31 and architects to perform acoustical measurements since the very early research and development  
32 phase, leading to an overall reduction of design costs and improved product quality.

33

34 *Keywords:* Acoustic measurements; Sound absorption coefficient; Measurement uncertainty;  
35 Building materials; Sustainability; Small-scale reverberation room.

36

37 **1. Introduction**

38 The design process of sound absorptive materials is complemented by a preliminary exploratory  
39 phase that requires an immediate feedback on the acoustic performance, i.e. the absorption  
40 coefficient. Therefore, adequate tools are needed to accelerate the research and development process,  
41 minimize costs, and reduce waste due to dismantled samples after their characterization. The  
42 absorption coefficient measurement procedure has been the focus of continuous research that have  
43 led to two main standardized methods, i.e. the impedance tube (IT) method defined in ISO 10534 [1]  
44 and the full-scale reverberation room (FSRR) method described in ISO 354 [2] and ASTM Standard  
45 C423 [3]. However, these methods present several disadvantages: IT does not allow to test 3D  
46 systems, while FSRR requires large samples. This paper aims to explore the capabilities of small-  
47 scale reverberation rooms (SSRR) in providing accurate estimations of the absorption coefficients  
48 with respect to the FSRR benchmarking and in overcoming the above-mentioned drawbacks of  
49 existing methods.

50 The main advantages of a SSRR are the possibility to test samples that are much smaller than 10-  
51 12 m<sup>2</sup> and the 6.69 m<sup>2</sup> recommended by the FSRR measurements ( $V > 200 \text{ m}^3$ ) according to ISO 354  
52 [2] and ASTM Standard C423 [3], respectively, and to allow more acousticians, manufacturers and  
53 practitioners to build their test facility due to the more feasible construction compared to a FSRR.  
54 This, in turn, enables a dramatic reduction of economical and time efforts necessary to perform a  
55 FSRR measurement. Moreover, the SSRR can be used to improve the quality of acoustic simulations:  
56 novel materials at configurations not available in existing databases can be characterized much more  
57 easily [4].

58 Due to their cost effectiveness, SSRRs have been the focus of research in the automotive sector [5],  
59 which usually requires absorption data at medium-high frequencies due to the small size of the  
60 involved samples. The research has led to a SAE (Society of Automotive Engineers) standard [6] on  
61 the use of small rooms for absorption coefficients measurements. The common size of these rooms

62 is in the range of 3-10 m<sup>3</sup>, and a sample area of 0.4-1.5 m<sup>2</sup> is usually deployed [7]: this leads to nearly  
63 90% reduction of the wasted material for laboratory measurements compared to the FSRR (12 m<sup>2</sup>).  
64 The sample arrangement in the SSRR requires a shorter set-up time: a single panel is usually  
65 sufficient, while in FSRR several panels need to be assembled to reach a 12 m<sup>2</sup> sample. In turn the  
66 transportation costs and the related environmental pollution benefit from the reduction in material  
67 volume. Moreover, the same samples could be reused to measure other important properties for  
68 building materials, e.g. the thermal conductivity [8], since the required sample dimensions are  
69 comparable to those used in small-scaled rooms.

70 Further SSRRs are reported in Rey et al. [9] with a volume of 1.12 m<sup>3</sup> and test sample area of 0.3 m<sup>2</sup>,  
71 and Pacheco et al. [10] with a volume of 0.96 m<sup>3</sup> and test sample area of 0.3 m<sup>2</sup>. These scaled rooms  
72 have been useful also for testing more complicated structures, e.g. 3D rigid polyester systems, which  
73 is difficult to test in an impedance tube [11]. The continuous research on SSRRs has led to the Alpha  
74 Cabin, built by the Swiss company Rieter, with a volume of 6.5 m<sup>3</sup>. The design and size of the Alpha  
75 Cabin is 1:3 scale of the large reverberation room located in the Swiss Federal Laboratory of Material  
76 Testing and Research Institute (EMPA). It is largely used in the automotive industry allowing to  
77 measure 1.2 m<sup>2</sup> of flat samples or 3D moulded finished parts providing accurate measurements in the  
78 frequency range of 400-5000 Hz [11].

79 A few studies have also compared small-scale reverberation room measurements with those  
80 performed in a full-scale reverberation room [9, 11-13]. A good match of the results has been shown  
81 in the range of frequencies above 400 Hz, where the SSRR is expected to fulfil the perfect diffusion  
82 conditions, i.e. where the degree of diffusion is close to 1. However, these studies also highlight larger  
83 discrepancies at low frequencies due to the reduced size of the room. This is a critical aspect since  
84 the resulting smaller sample area with equal height produces a larger edge effect [14, 15]. The impact  
85 of these effects is particularly high at low frequencies if highly absorbing materials with high  
86 thicknesses are tested.

87 Therefore, two main concerns appear when dealing with small reverberation rooms. The first is  
88 related to the lack of a degree of diffusivity of the sound field required to make the measurement  
89 conditions largely independent of the room properties [16]. To mitigate this issue, usually different  
90 types of diffusers are introduced [2, 17,18]; nevertheless, the efficiency of the diffusers is shown to  
91 be reduced when the frequency decreases [19]. In addition, according to Scrosati et al. [20], the  
92 diffusers change the mean free path in the reverberation room, thus ISO 354 formula for the  
93 calculation of the equivalent absorption area is no longer valid since it does not take into account the  
94 actual mean free path and consequently the changed volume of the room. However, low diffusivity  
95 of reverberation rooms is still one of the main concerns of the ISO 354 measurements related to the  
96 low reproducibility values among laboratories. This is much evident at low frequencies [21], but  
97 appear even above the Schroeder frequency, where the sound field should reach a higher degree of  
98 diffusivity [22, 23]. One of the causes is due to the fact that the sound field is diffuse in the empty  
99 room, while in the room with a highly absorbing sample the sound field cannot be considered  
100 perfectly diffuse [20]. For this reason, the diffuse field conditions differences among laboratories has  
101 been questioned lately aiming at new requirements to be defined in terms of diffusivity for qualified  
102 laboratories [24]. Several studies have shown that large discrepancies might occur among different  
103 full-scale laboratories even though they fulfil the ISO qualification requirements [25]. As for FSRR,  
104 the low frequencies range in SSRR is the most critical one, where the early decay is dependent on  
105 strong, distinct reflections and need to be treated with specific methods [26, 27].

106 The second drawback of SSRR measurements is related to the diffraction due to the finite size of the  
107 tested material, especially at the low frequencies, which is known as the edge effect [14, 28, 29], and  
108 restricts the reliability frequency range at medium-high frequencies. Further investigation is needed  
109 to clarify the trade-off between reduced sample size and the appropriate room and sample conditions  
110 to obtain reliable results for building materials.

111 To shed light in this direction, this study examines a broad measurement campaign in a small-scale  
112 reverberation room in the laboratories of the Department of Energy (DENERG) of Politecnico di  
113 Torino, with the aim to evaluate the reliability of the sound absorption coefficient measurements.  
114 Four different materials at three different sizes and orientations on the room floor have been tested.  
115 The work assesses the compatibility of the SSRR measurements towards measurements made on the  
116 same materials in a full-scale reverberation room (ISO 354) [2] at INRiM (Istituto Nazionale di  
117 Ricerca Metrologica). Moreover, the same materials have been additionally characterized with the  
118 impedance tube method (ISO 10534-2) [1] in order to present an easier and direct comparison towards  
119 another standardized method. Finally, the single sound absorption indices  $\alpha_w$  (weighted sound  
120 absorption coefficient), NRC (Noise Reduction Coefficient), and SAA (Sound Absorption Average),  
121 which are used to assess the quality of the absorption and to select products by designers and  
122 architects, are derived from the three measurement methods.

## 123 **2. Methods**

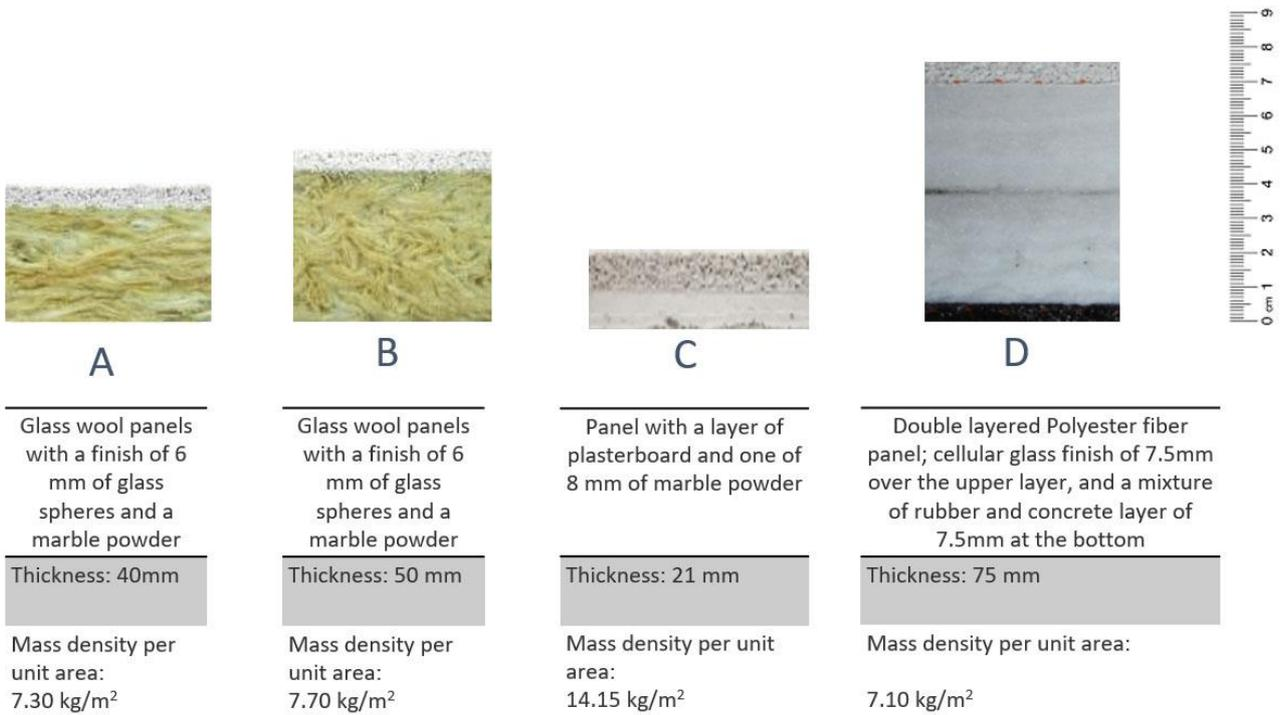
124 The research has been organized through the following steps:

- 125 1) Selection of materials and preparation of samples for the measurements in IT, FSRR and  
126 SSRR;
- 127 2) Measurement of sound absorption in the IT according to ISO 10534-2 [1] and FSRR according  
128 to ISO 354 [2];
- 129 3) Measurement of sound absorption in the SSRR and test the range of application of ISO 354  
130 [2] method by varying the area of the sample and its orientation on the room floor;
- 131 4) Evaluation of the compatibility of the measured SSRR data with the results from IT and  
132 FSRR;
- 133 5) Computation of the indices  $\alpha_w$ , SAA and NRC for the IT, FSRR and SSRR data and  
134 compatibility assessment.

135

136 2.1 Tested Materials

137 Four materials (here labelled A, B, C, D) available at INRiM have been tested (Figure 1). Materials  
 138 A and B are made of glass wool panels with a density of  $80 \text{ kg/m}^3$  and a 6 mm finished layer made  
 139 of glass spheres and a marble powder with overall thickness of 40 mm and 50 mm, respectively.  
 140 Material C is a 21 mm thick panel with a layer of 13 mm of plasterboard and 8 mm finished layer  
 141 made of a marble powder. Material D is composed of two superimposed layers of polyester fibre with  
 142 a density of  $80 \text{ kg/m}^3$  and a thickness of 30 mm each. Also, this material has a cellular glass finish of  
 143 7.5 mm over the upper layer, and a mixture of rubber and concrete layer of 7.5 mm at the bottom.  
 144 Since all these materials are obtained by layers of different characteristics, they can be considered as  
 145 non-isotropic. The four materials have been chosen based on commercially available materials in  
 146 order to have four different thicknesses: two similar materials A and B with the same layers  
 147 characteristics but with slightly different thickness, material C considered as a thin rigid material and  
 148 material D was chosen in order to test the SSRR also for significant thicknesses.



149

150 **Fig. 1.** Sample A and B: Glass wool panels with a finish of glass spheres and a marble powder (40  
151 mm and 50 mm). Sample C: one layer of plasterboard and one of marble powder (21 mm). Sample  
152 D: Double layered polyester fibre panel with a cellular glass finish (75 mm).

153

## 154 2.2 Impedance tube measurements

155 Measurements have been performed in the impedance tube in accordance with ISO 10534-2 [1] (two-  
156 microphone technique) in order to measure the normal-incidence absorption coefficient ( $\alpha_0$ ) for the  
157 four materials. The advantages of this method rely on the possibility to obtain measurements using  
158 small samples of less than  $0.1 \text{ m}^2$  that are easily obtained and introduced into the impedance tube.  
159 These measurements took place in the INRiM laboratory. Two different tubes of 30 mm and 50 mm  
160 diameter each (Figure 2), both equipped with two  $\frac{1}{4}$ " microphones (Brüel & Kjær 4136), have been  
161 used in order to assure a higher accuracy in the whole frequency range of interest, i.e. 100-5000 Hz.  
162 The 30 mm tube (length of 45 cm and microphone spacing of 16 mm) allows to measure with a high  
163 accuracy in the frequency range of 400-6300 Hz and the 50 mm tube (length of 52 cm and microphone  
164 spacing of 26 mm) in the frequency range of 100-3150 Hz. The ISO 10534-2:2001 standard does not  
165 define the exact frequency range for a given tube diameter and microphone separation, but  
166 recommends the bounds for the lower and upper frequencies; therefore, the frequency range was  
167 chosen to satisfy the standard requirements for the level of nonlinearities, frequency resolution,  
168 measurement instabilities and signal-to-noise ratio [30].

169 Both the two tubes are equipped with a white noise source which generates a flat spectrum in the 100-  
170 5000 Hz frequency range. The possible gaps among the sample perimeter and the tubes inner surfaces  
171 have been sealed by covering the sample border with vaseline without creating local compression on  
172 the samples. In this way, the size of the voids between the tested material and the sample holder was  
173 reduced so that the circumferential effect discussed in [31] could be considered negligible. The effect  
174 of the irregularities in the samples, and in particular at the edges, was taken into consideration by

175 repeating the tests with three different samples. Temperature and atmospheric pressure were  
176 measured with proper calibrated transducers. For each material type, measurements were performed  
177 on three samples (nominally equal), obtained from the same larger sample, in order to evaluate  
178 uncertainty contribution due to reproducibility.

179 The normal-incidence absorption coefficients ( $\alpha_0$ ) data from the two tubes measurements have been  
180 combined in order to fulfil their covered frequency range, thus considering the values from the 50  
181 mm tube in the range 100-315 Hz; the mean values from the two tubes in the range 400-3150 Hz and  
182 the values from the 30 mm tube in the range 4000-5000 Hz. These data are shown in Appendices A,  
183 B, C and D as  $IT_n$ .

184 These values have been corrected for diffuse incidence based on the approach proposed in Spagnolo  
185 and Benedetto [32], which uses a physical model to determine the random-incidence absorption  
186 coefficient ( $\alpha$ ) by integrating a vector of evenly spaced 90 angles between  $0^\circ$  and  $90^\circ$ , i.e. the whole  
187 hemi-solid angle, allowing to estimate the sound energy density absorption at each angle of incidence,  
188 randomly, as in near-diffuse field, according to Eq. (1). There are several methods that can be used  
189 to perform this correction taking into account the finite sample size [xx] and a different angular  
190 integration limit [xx].

$$\alpha = \int_0^{\pi/2} \alpha_\theta \cos\theta \, d\theta \quad (1)$$

191

192 where  $\theta$  is the angle of incidence of the pressure waves on the sample and  $\alpha_\theta$  is the sound absorption  
193 coefficient at angle  $\theta$  given by Eq. (2);

$$\alpha_\theta = 1 - \left| \frac{Z \cos\theta - \rho_0 c}{Z \cos\theta + \rho_0 c} \right|^2 \quad (2)$$

194

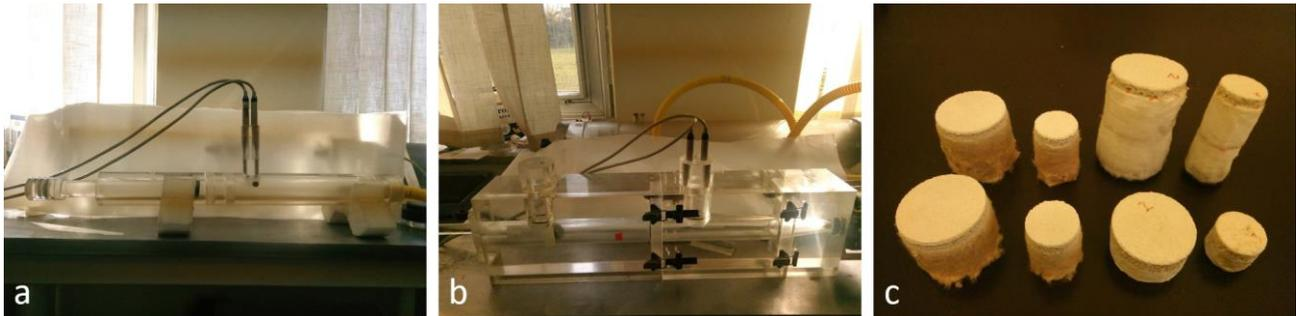
195 where  $Z$ , assuming locally reacting surface, is the acoustic impedance of the absorbing material given  
196 by:

$$Z = \rho_0 c \frac{1 + (1 - \alpha_0)^{1/2}}{1 - (1 - \alpha_0)^{1/2}} \quad (3)$$

197

198 where  $\rho_0$  is the density of air,  $c$  is the speed of sound, and  $\alpha_0$  is the normal-incidence absorption  
 199 coefficient evaluated in the impedance tube.

200



201

202 **Fig. 2.** Measurements set-up in the impedance tube with a diameter of a) 30 mm and b) 50 mm, and  
 203 c) circular samples of the four materials with a diameter of 30 and 50 mm.

204

### 205 2.3 Full-scale reverberation room measurements

206 All the materials have been tested in the full-scale reverberation room at INRiM, which is a qualified  
 207 room for measurements in accordance with ISO 354 [2]. The method allows to estimate the random-  
 208 incidence absorption coefficient ( $\alpha_s$ ) in the 100-5000 Hz frequency range. The room has a floor  
 209 surface of 59.4 m<sup>2</sup> and a height of 4.95 m, which lead to a volume of 294 m<sup>3</sup>. Room plan is irregular  
 210 with non-parallel side walls. The indoor surfaces are characterized by strongly reflective walls and a  
 211 marble floor characterized by an equivalent sound absorption area lower than 5 m<sup>2</sup> in the 100-5000  
 212 Hz frequency range. The mean reverberation time of the empty room between 100 Hz and 5000 Hz  
 213 is of 10.3 s, thus the Schroeder frequency  $f_s$  is 374 Hz. Five diffusers are hung over the ceiling in  
 214 order to assure diffusivity. The tested samples have an area of 12 m<sup>2</sup> and have been located on the  
 215 floor of the room within a wooden frame, which is recommended to be used to seal the edges of the  
 216 tested material. In this experiment the frame has been used for all the samples except for the case of

217 sample C, which has a negligible thickness. The porous layer for this material is of 8 mm, which was  
218 taken into account in the estimation of the overall area of the sample by increasing it of 0.11 m<sup>2</sup>.

219 The set-up and the samples of each material have been arranged in accordance with the  
220 recommendations of the ISO 354 standard (Figure 3):

- 221 • microphones should be positioned at a minimum distance of 1.5 m from each other, 1 m from  
222 the room surfaces and 2 m from the sources;
- 223 • the two sources must be at least 3 m apart from each other. A spatial averaging is performed  
224 considering all the 12 sources and microphones combination;
- 225 • the interval of frequencies of interest is reported as third-octave bands in the range 100-5000  
226 Hz;
- 227 • controlled conditions of temperature (> 15 °C) and humidity (between 30-90 %);
- 228 • the sample must be rectangular with a ratio between width and length within the range 0.7-1.  
229 In this specific case, the test specimens were composed of 25 single small panels with size  
230 60×80 cm<sup>2</sup> combined in order to cover an area of 4×3 m<sup>2</sup>;
- 231 • the sides of the sample must be distant from the walls of the room by at least 1 m.

232



233

234 **Fig. 3.** Measurements in the full-scale reverberation room a) without and b) with the sample.

235

236 The procedure consists in using the interrupted noise method [2] on six different microphone  
 237 positions in two conditions, i.e. with and without the sample on the floor of the room. The  
 238 measurement chain is composed of a 1/2" microphone (Brüel & Kjær 4943), sequentially located at  
 239 different positions, and two dodecahedral sources (Brüel & Kjær 4292 and Brüel & Kjær 4296). The  
 240 applied recording system is the SINUS, Apollo system with software Samurai 2.6; while the sound  
 241 equalizer is Yamaha (DEQ 5) and the power amplifier is Amcron Crown (MICRO-TECH 1200). In  
 242 these measurements two sound sources are used for the simultaneous excitation, therefore the number  
 243 of spatially independent measured decay curves may be reduced to six [2]. For each of the six  
 244 positions, measurements are repeated four times, and the reverberation time relative to a 20 dB decay,  
 245 i.e.  $T_{20}$ , is evaluated and used to estimate the  $T_{60}$ , i.e. the reverberation time occurring for a 60 dB  
 246 decay. The data are spatially averaged with the ensemble averaging method in order to obtain  $T_1$  and  
 247  $T_2$  without and with the sample on the room floor, respectively. The difference between the two  
 248 measures is used to calculate the variation of the equivalent sound absorption area  $A_T$  based on  
 249 Sabine's theory:

$$A_T = 55.3V \left( \frac{1}{c_2 T_2} - \frac{1}{c_1 T_1} \right) - 4V(m_2 - m_1) \quad (4)$$

250  
 251 where  $T_1$  and  $T_2$  are the reverberation times of the empty reverberation room and after the test  
 252 specimen has been introduced, respectively;  $V$  is the volume of the empty reverberation room;  $c_1$  and  
 253  $c_2$  is the propagation speed of sound in air in the room without the sample:  $c_1 = 331 + 0,6 t_1$ ,  $t_1$  is the  
 254 air temperature;  $m_1$  and  $m_2$  is the power attenuation coefficient of the climatic conditions in the  
 255 reverberation room without and with the sample (calculated according to ISO 9613-1 [33]);

256  
 257 The random-incidence absorption coefficient is defined as:

$$\alpha_s = \frac{A_T}{S} \quad (5)$$

258

259 Where  $S$  is the area covered by the test sample.

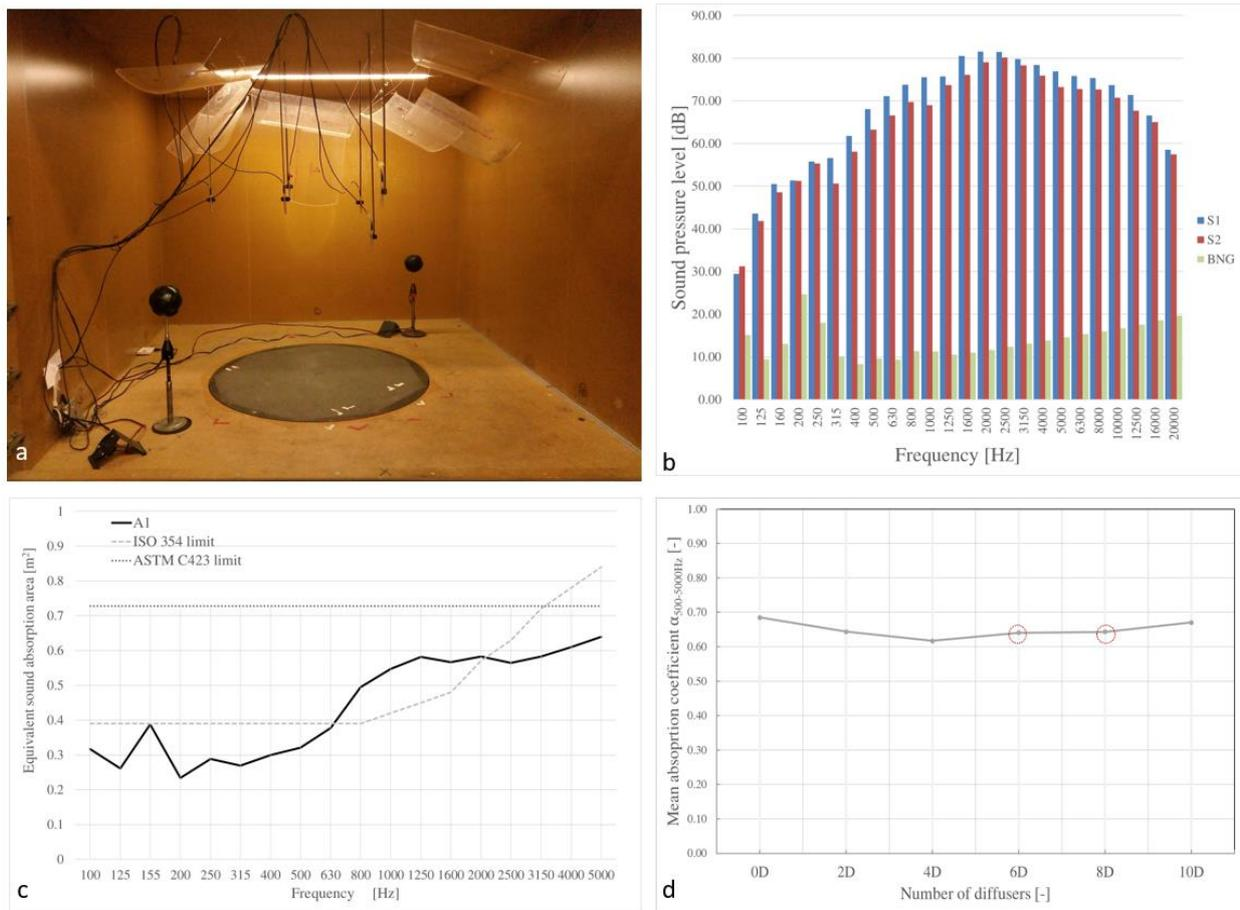
260

#### 261 2.4 Small-scale reverberation room measurements (SSRR)

262 The small-scale reverberation room (Figure 4, a and Figure 5) is a laboratory at DENERG  
263 (Department of Energy, Politecnico di Torino, Italy). It is a 1:5 scale reproduction of the reverberation  
264 room described above. The room has been primarily built for random-incidence scattering coefficient  
265 measurements according to ISO 17497-1 [34, 35]. It is an oblique angled room with pairs of  
266 nonparallel walls. The floor area is about 2.38 m<sup>2</sup> and the height in the range 1-1.2 m, which lead to  
267 a maximum volume of 2.86 m<sup>3</sup> and a total area of 12.12 m<sup>2</sup>. The structure is raised from the ground  
268 on a wooden structure and damping layers have been used along the joints and openings. One of the  
269 sides consists of two movable parts that allow to have a large opening to ease the positioning of the  
270 sample. The construction material is self-supporting lightweight partitions of MDF (Medium Density  
271 Fibreboard) with a thickness of 3.8 cm, which has been further covered by a layer of adhesive film in  
272 order to maximize its reflective properties. The equivalent sound absorption area of the empty room  
273 ( $A_1$ ) and ISO [2] and ASTM [3] limits are shown in Figure 4, c. The ISO limit values have been  
274 multiplied by the factor  $(V/200)^{2/3}$ , while the ASTM limit value is given in terms of mean absorption  
275 coefficient ( $\alpha_m=0.06$ ) and has been converted into equivalent sound absorption area for comparison  
276 purposes. Given that the ISO limit is not specifically indicated for rooms below a volume of 150 m<sup>3</sup>,  
277  $A_1$  can be considered acceptable even though slightly above the limit in the range 800-1600 Hz.  
278 However, the average absorption coefficient of the indoor surfaces is lower than  $\alpha_m=0.05$  in the  
279 frequency range of interest (100-5000 Hz). The mean reverberation time of the empty room between  
280 100 Hz and 5000 Hz of 0.95 s, thus the Schroeder frequency  $f_s$  is 1152 Hz.

281 In order to assure a high diffusivity of the sound field [36], 8 diffusers (13.5% of the total room area)  
282 have been hung over the ceiling, which is considered as a more economical solution compared to  
283 boundary diffusers leading to an almost equivalent effect on the diffusion of the sound field [18]. A  
284 systematic study of the sound field diffusivity evaluation of the room has been performed in [37].

285 The diffusivity check has been performed in accordance with ISO 354 based on the measurements of  
 286 the mean absorption coefficient (500-5000 Hz) of a highly sound absorptive panel made of 5 cm thick  
 287 polyester fibre (Figure 4, d). The final number of diffusers was set to 8, which was a compromise  
 288 between the rule set by the standard i.e. the mean sound absorption coefficient approaches a constant  
 289 value (6D to 8D), and limited effect on the volume reduction of the room due to the total coverage of  
 290 the ceiling, i.e the condition with 10 diffusers (10D).



291  
 292 **Fig. 4.** a) Empty small-scale reverberation room; b) spectral characteristics of the two sound sources  
 293 (S1 and S2) and background noise; c) comparison of the equivalent sound absorption area of the  
 294 empty room ( $A_1$ ), ISO and ASTM limits; d) mean absorption coefficient of a polyester panel of 5 cm  
 295 measured in the room with no diffusers (0D) and 2-10 diffusers (2D-10D).

296

297 The procedure consists in using the integrated impulse response method [2] for simultaneous  
298 measurements on six different microphone positions in two conditions, i.e. with and without the  
299 sample on the floor of the room as in section 2.3. The measurement chain is composed of six 1/4”  
300 BSWA Tech MPA451 microphones and ICP104 (BSWA Technology Co., Ltd., Beijing, China); two  
301 ITA High-Frequency Dodecahedron Loudspeakers with their specific ITA power amplifiers (ITA-  
302 RWTH, Aachen, Germany) and a sound card Roland Octa-Capture UA-1010 (Roland Corporation,  
303 Japan) in order to perform 12 measurements (the minimum number required by ISO 354 [2]). The  
304 software used for the measurements, i.e. sound generation, recording and signal processing, is  
305 MATLAB combined with the functions of the ITA-Toolbox (an opensource toolbox from RWTH-  
306 Aachen, Germany) [38]. The sound source should fulfil the ISO 354 spectral characteristics, that is,  
307 the sound pressure levels in the room shall be less than 6 dB in adjacent one-third-octave bands and  
308 the level of the excitation signal before the decay shall be sufficiently high so that the lower decibel  
309 level of the evaluation range is at least 10 dB above the background noise level, i.e. 35 dB below the  
310 initial sound pressure level. The first criterion is fulfilled for the entire frequency range, while the  
311 second is fulfilled only above the 250 Hz (Figure 4, b).

312 For each of the 12 measurements the reverberation time is evaluated. The data are spatially averaged  
313 in order to obtain  $T_1$  and  $T_2$  without and with the sample on the room floor, respectively. Equations  
314 4 and 5 are then applied to estimate the random-incidence absorption coefficient.

315 The set-up and the samples of each material have been arranged in agreement with the  
316 recommendations of the ISO 354 standard (Figure 5):

- 317 • “microphones should be positioned at a minimum distance of 1.5 m from each other, 1 m  
318 from the room surfaces and 2 m from the sources”. This leads to 0.3 m; 0.2 m and 0.4 m in  
319 1:5 scale;
- 320 • “the two sources must be at least 3 m apart”. This leads to 0.6 m in 1:5 scale. A spatial  
321 averaging is performed considering all the 12 sources and microphones combination;

- 322 • the frequencies of interest are reported as third-octave bands in the range 100-5000 Hz. Given  
323 the background noise criterion, this is valid for 250-5000 Hz;
- 324 • controlled conditions of temperature ( $> 15\text{ }^{\circ}\text{C}$ ) and humidity (between 30-90 %). A sensor has  
325 been installed inside the room;
- 326 • “the sides of the sample must be distant from the walls of the room by at least 1 m”. This leads  
327 to 0.2 m in 1:5 scale;

328

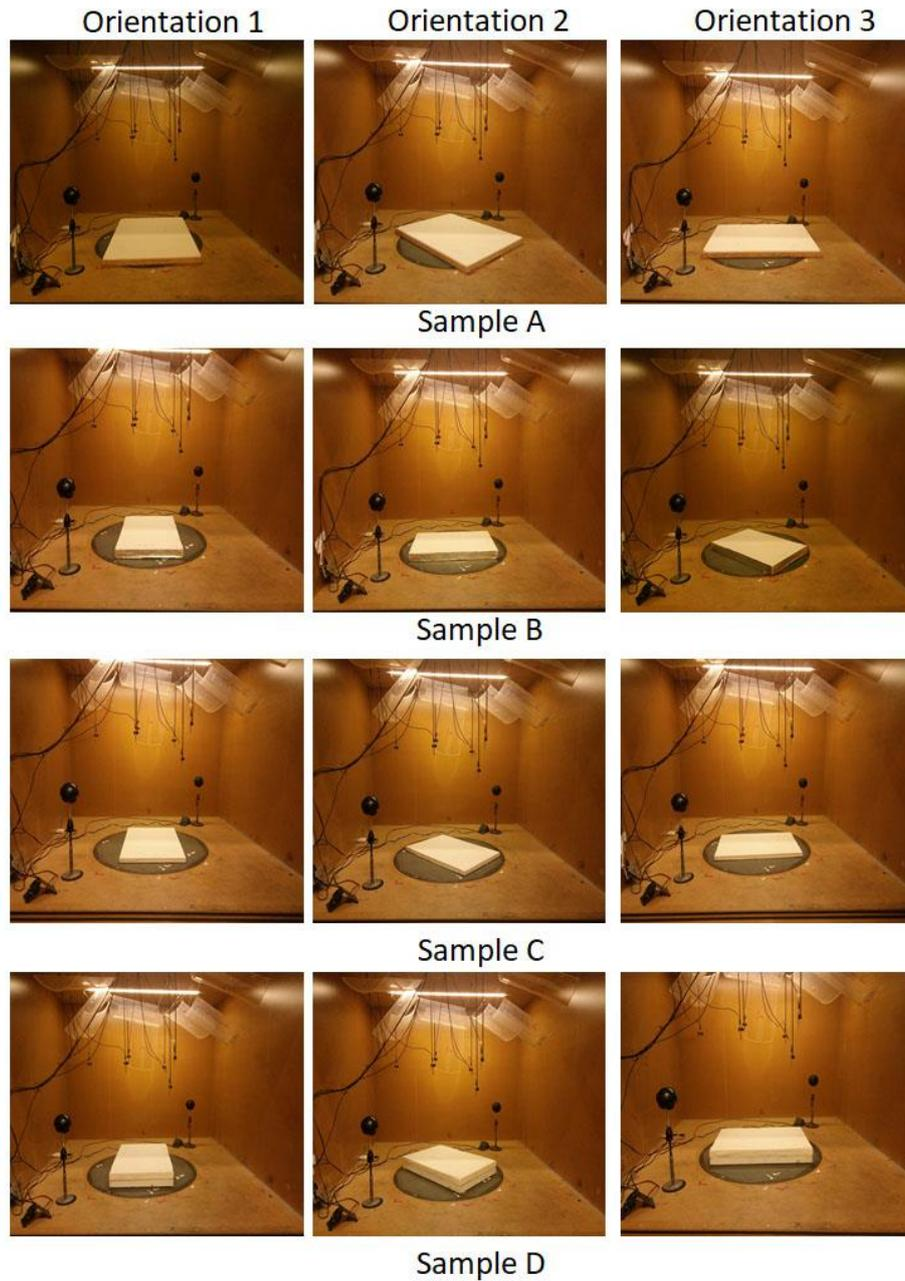
#### 329 2.4.1 Sample configuration

330 One of the aims of this study is to define the sample configuration that could lead to accurate results  
331 of the absorption coefficient measurements in the small-scale reverberation room. Given the small  
332 size of the SSRR, the sound field is expected to be strongly dependent on the configuration of the  
333 measured material. Therefore, it is crucial to define the application range of this type of  
334 measurements.

335 The following variables have been considered, tested and the results have been compared with the IT  
336 and FSRR measurements:

- 337 - three different sample sizes for each material ( $60\times 40\text{ cm}^2$ ;  $60\times 60\text{ cm}^2$ ; and  $60\times 80\text{ cm}^2$ ). It  
338 should be noted that the ISO 354 recommends a ratio between width and length in the range  
339 0.7-1;
- 340 - three different orientations on the floor (Fig.5) for the  $60\times 40\text{ cm}^2$  and  $60\times 80\text{ cm}^2$  sample sizes  
341 and two different orientations for sample  $60\times 60\text{ cm}^2$ . Orientation 1 assumed the long edge of  
342 the sample parallel to the side wall, orientation 2 assumed the axis of symmetry of the sample  
343 aligned over the diagonal of the room floor giving an oblique orientation, and orientation 3  
344 assumed the long edge of the sample parallel to the rear wall. It should be noted that the ISO  
345 354 standard recommends an oblique orientation (orientation 2).

346 Three repetitions have been performed for each configuration.



347

348 **Fig. 5.** Measurements in the small-scale reverberation room of one of the samples with three different  
 349 orientations; Sample A ( $60 \times 80 \text{ cm}^2$ ), Sample B ( $60 \times 40 \text{ cm}^2$ ), Sample C ( $60 \times 40 \text{ cm}^2$ ) and Sample D  
 350 ( $60 \times 40 \text{ cm}^2$ ).

### 351 **3 Analyses**

352 An analysis based on the estimation of the normalized error ( $E_n$ ) has been performed in order to assess  
 353 the compatibility of the absorption coefficient data measured in the SSRR with respect to the FSRR

354 ( $E_{n,FSRR}$ ), considered as reference value for random incidence sound absorption, and IT extended for  
355 random-incidence absorption coefficients ( $E_{n,IT}$ ). Moreover, also the normalized error of IT results  
356 has been assessed with respect to the FSRR values.  $E_n$  is defined as the ratio of the difference between  
357 the reference value ( $\alpha_x$ ) and the reported value ( $\alpha_y$ ) compared to the root sum square of associated  
358 expanded uncertainties ( $U_x$  and  $U_y$ ) at a confidence level of 95% ( $k=2$ ). According to ISO/IEC  
359 17043:2010 [39], it is evaluated as follows:

$$E_n = \frac{|\alpha_x - \alpha_y|}{\sqrt{U_x^2 + U_y^2}} \quad (6)$$

360

361 The data can be considered compatible when  $E_n < 1$ . This is an indicator of accuracy/inaccuracy as  
362 compared to an assigned reference value (FSRR or IT) with respect to the associated uncertainties.

363 The uncertainty of the impedance tube measurements has been assessed according to GUM-JCGM  
364 100:2008 [40]), taking into account, as type B uncertainty contribution, the difference between the  
365 maximum and minimum values coming from the measurement on three nominally equal samples  
366 with a uniform rectangular distribution. The specific guidelines given by Wittstock (2018) (see Eq.  
367 (2) and Table II – smooth case) [41], which are currently the most reliable reference for the  
368 uncertainty evaluation in reverberation rooms based on a database of Interlaboratory Tests, have been  
369 applied for the SSRR and FSRR measurement uncertainties. Nevertheless, as shown by the author  
370 itself [41], larger uncertainties might occur, especially for highly absorptive materials with ISO 354  
371 method, thus entailing a possible underestimation of the  $E_n$  values. Such aspect should be taken into  
372 account in the conclusions. The measured frequency dependent absorption coefficients of the four  
373 materials and the estimated measurement uncertainties are shown for further details in Appendices  
374 A, B, C and D.

375 The normalized error data have been further analysed with a focus on the effects of the independent  
376 factors, i.e. the sample size and orientation. The SPSS Statistics software [42] has been used to  
377 perform the ANOVA (ANalysis Of VAriance). The data have been first analysed with a normality

378 test (Kolmogorov-Smirnov test):  $E_{n,IT}$  showed a skewness of 0.793 (std.error = 0.105) and kurtosis of  
 379 0.004 (std.error = 0.210);  $E_{n,FSRR}$  showed a skewness of 0.793 (std.error = 0.105) and kurtosis of 0.004  
 380 (std.error = 0.210), thus falling within the acceptable range of  $\pm 2$  [42].

381 Moreover, the single indices for sound absorption ( $\alpha_w$ , NRC and SAA) are derived from the IT, FSRR  
 382 and SSRR measurements and compared in terms of compatibility.

383

384 Table 1: ANOVA results for  $E_{n,IT}$  and  $E_{n,FSRR}$  data set.

Material	$E_{n,IT}$				$E_{n,FSRR}$			
	Size		Orientation		Size		Orientation	
	F	p	F	p	F	p	F	p
A	(2, 135) 21.580	0.000	(2, 135) 0.095	0.910	(2, 135) 15.248	0.000	(2, 135) 0.110	0.896
B	(2, 135) 13.910	0.000	(2, 135) 0.093	0.980	(2, 135) 5.496	0.005	(2, 135) 0.090	0.914
C	(2, 135) 0.827	0.440	(2, 135) 0.468	0.628	(2, 135) 0.501	0.607	(2, 135) 0.235	0.791
D	(2, 135) 5.481	0.005	(2, 135) 0.308	0.736	(2, 135) 20.018	0.000	(2, 135) 0.255	0.776

385

## 386 4 Results and discussion

### 387 4.1 Effects of the independent factors

388 The ANOVA performed on the overall  $E_n$  set of data showed that the four materials are significantly  
 389 different from each other at a confidence level of 95% for  $E_{n,IT}$  with respect to IT ( $F(3, 540) = 14.143$   
 390 and  $p < 0.001$ ) and at a confidence level of 90% for  $E_{n,FSRR}$  with respect to FSRR ( $F(3, 540) = 2.277$

391 and  $p = 0.079$ ). Therefore, sample size and orientation variables have been analysed for each material  
392 separately (Table 1).

393 The effect of the sample size is statistically significant for all the samples typologies ( $p < 0.05$ ), except  
394 for sample C. This result might be due to the limited edge effect for thinner samples, as sample C is  
395 21 mm thick. Appendices A, B, C and D show the absorption coefficient values for each material.  
396 For panels with higher thickness (i.e. A, B, D) and when the panel reaches the smallest dimensions  
397  $60 \times 40 \text{ cm}^2$ , there are evident irregular high peaks at mid and high frequencies for panels A and B,  
398 and also at low and mid frequencies for panel D. It can be noticed that the sound absorption increases  
399 at 160-400 Hz and above 800 Hz with decreasing samples size (Appendices A, B, and D). This  
400 behaviour might be due to a combination of edge effects and to diffusivity effects, caused by the  
401 influence of the material on the modal behaviour of the room with and without the sample inside, whereas  
402 for low absorbing materials (Appendix C) it can be considered equivalent in terms of spatial distribution  
403 and amplification of standing waves. Schiavi and Prato [43] showed these discrepancies by comparing  
404 full scale reverberation room, impedance tube, and airflow resistivity methods. The same result has  
405 been highlighted also in full-scale rooms by Jain et al. [44], for samples size smaller than  $1 \text{ m}^2$ , which  
406 is due to diffraction occurring at the sample edges. Anyway, in general terms, depending on the  
407 sample thickness, the small room gives higher sound absorption values as compared to large  
408 reverberation rooms [15]. Samples A, B and D showed this trend above 800 Hz, while sample C  
409 above 2000 Hz.

410 The correct scaling of the sample size with respect to the room volume has been investigated also in  
411 Veen et al. [28]. This study shows that a sample of  $1.12 \text{ m}^2$  could be considered in order to have  
412 reliable results in a small reverberation room with a volume of about  $6.4 \text{ m}^3$ . The ratio between the  
413 room volume and the sample area is comparable to the one obtained with the room volume of  $2.86 \text{ m}^3$   
414 and the sample size  $60 \times 80 \text{ cm}^2$  ( $0.48 \text{ m}^2$ ) used in the present study (i.e. ratio  $\approx 6$ ).

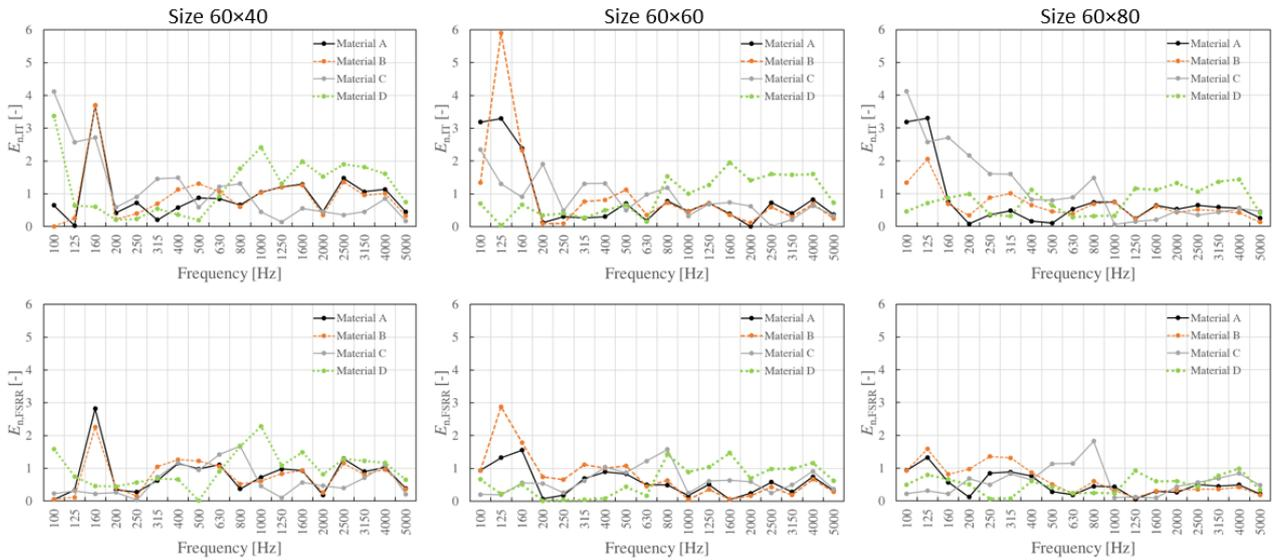
415 The effect of the sample orientation has been analysed for all the materials and all the sample sizes.  
416 Table 1 shows that the differences due to sample orientations are not statistically significant for all  
417 the materials considered ( $p > 0.05$ ). It is therefore possible to choose an oblique panel orientation  
418 (Orientation 2), as suggested in the standard for full-scale measurements. Previous research [16] has  
419 shown that different orientations may cause discrepancies at lower frequencies (below 400 Hz) and  
420 that the smoothest curve is obtained for the oblique orientation, which is the most asymmetric one.  
421 This study also highlighted that the other two orientations cause strong peaks in the absorption  
422 coefficient, which were unrealistic for the tested porous materials. The authors argued that this  
423 behaviour might be due to the parallel orientation of two edges of the material against two side walls  
424 of the reverberation room. However, this effect is not fully observed in the study presented in this  
425 paper. Some differences between the three orientations are observed at specific frequencies for the  
426 smallest sample size, i.e.  $60 \times 40 \text{ cm}^2$  (Appendixes A, B, C, and D). Discrepancies at lower frequencies  
427 are reduced when the material has lower thickness, i.e. these differences are more evident in the case  
428 of panel D, which has a thickness of 75 mm. This finding is coherent with the results of Cops et al.  
429 [16], which showed the same discrepancies between different orientations for samples with thickness  
430 higher than 100 mm in full-scale measurements.

431

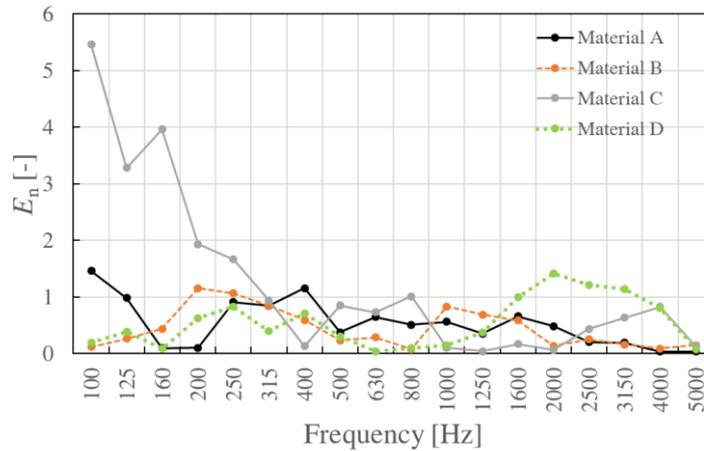
#### 432 4.2 Compatibility of SSRR with IT and FSRR data

433 Figure 6 shows the maximum normalized error values estimated in each third octave band frequency  
434 range for the SSRR data with respect to FSRR and IT data. SSRR data are reliable from 250 Hz  
435 upward, due to the background noise criterion previously discussed, however, for the sake of  
436 completeness, results are reported from 100 Hz. These plots show the  $E_n$  for material A, B, C and D  
437 at three sample sizes ( $60 \times 40 \text{ cm}^2$ ,  $60 \times 60 \text{ cm}^2$ , and  $60 \times 80 \text{ cm}^2$ ) and Orientation 2 only, since this  
438 factor was not found to be statistically significant. The results show that the normalized error ( $E_n$ ) is  
439 minimized for sample size  $60 \times 80 \text{ cm}^2$  for all the materials.  $E_{n,FSRR}$  values are lower than 1 in the

440 frequency range 400-5000 Hz, for materials A, B and D. Sample C presents  $E_{n,FSRR}$  values lower than  
 441 1 at 400 Hz and in the frequency range 1000-5000 Hz. Values slightly higher than 1 result between  
 442 500 Hz and 800 Hz. As highlighted in the previous section, this might be due to the limited effects of  
 443 this low absorbing and thinnest sample on the modal behaviour of the room it-self. This result  
 444 suggests further future investigation on the room diffusivity. The same conclusions can be obtained  
 445 for  $E_{n,IT}$  for materials A, B and C. For what concern material D, it can be noted that  $E_{n,IT} < 1$  only at  
 446 500-1000 Hz. This could be due to the fact that IT method tends to underestimate the sound absorption  
 447 at mid-high frequencies as shown in Appendix and in Figure 6.  $E_{n,IT}$  values are higher than  $E_{n,FSRR}$   
 448 values, which leads to a higher compatibility of the SSRR with respect to the FSRR. These differences  
 449 are maximized for the thickest material D, i.e.  $E_{n,IT} > 1$  and  $E_{n,FSRR} < 1$  at 1250-4000 Hz. The same  
 450 behaviour can be observed also when evaluating the normalized error of the IT data with respect to  
 451 the FSRR (Figure 7), i.e.  $E_n > 1$  at 1600-3150 Hz.



452  
 453 **Fig. 6.** Normalized error ( $E_n$ ) for SSRR results (material A, B, C and D) with respect to IT ( $E_{n,IT}$ ) and  
 454 FSRR ( $E_{n,FSRR}$ ) values for the three sample sizes ( $60 \times 40$  cm<sup>2</sup>,  $60 \times 60$  cm<sup>2</sup>, and  $60 \times 80$  cm<sup>2</sup>) and  
 455 orientation 2. The data can be considered compatible when  $E_n < 1$ .



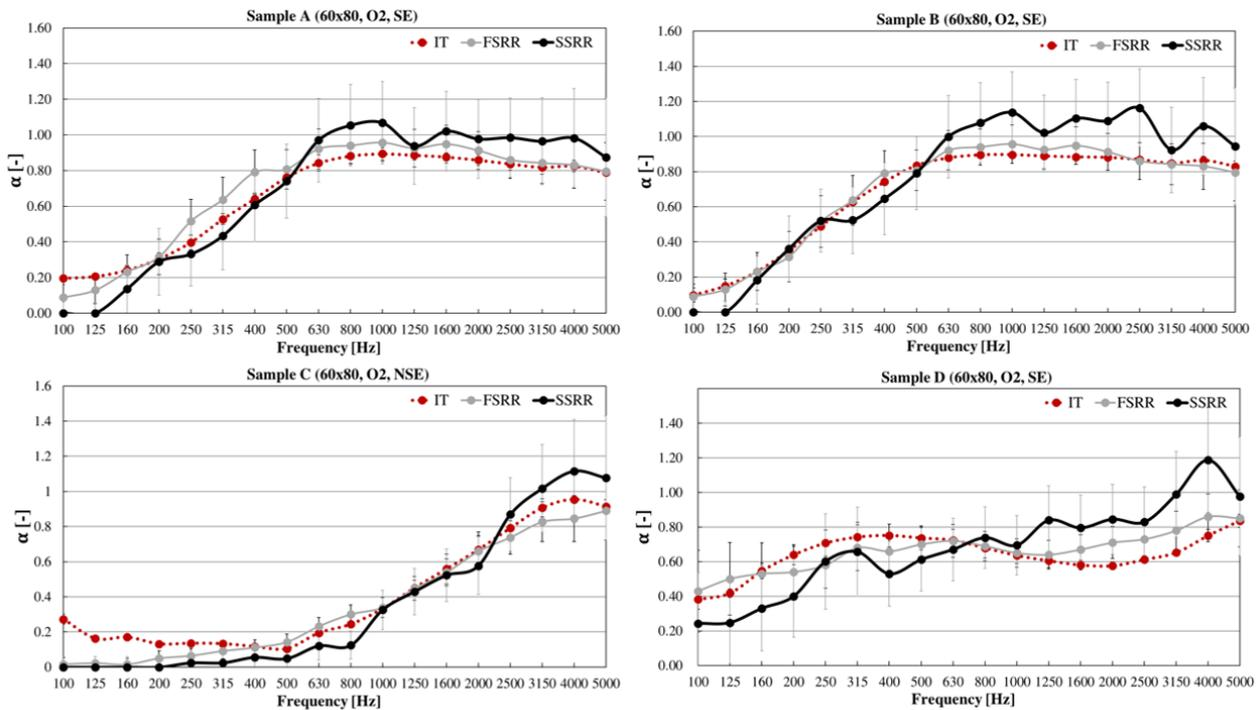
456

457 **Fig. 7.** Normalized error ( $E_n$ ) for IT results (material A, B, C and D) with respect to the FSRR values.

458 The data can be considered compatible when  $E_n < 1$ .

459

460 The absorption coefficient data of the optimal condition i.e. size  $60 \times 80$  cm<sup>2</sup> and sample orientation  
 461 2, together with the uncertainty values of the results, are shown in Figures 8. The plots show that the  
 462 SSRR values tend to be higher for frequencies above 800 Hz for samples A, B and D and above 2000  
 463 Hz for sample C. One of the causes for this behaviour is that the absorption coefficient approaches to  
 464 1 at these frequency ranges and influences the diffusivity of the sound field generated within the  
 465 small-scale room. This has been observed also in Veen et al. [28], where higher discrepancies around  
 466 1000 Hz for samples with thickness above 25 mm were found. Also, Jain et al. [44] showed a good  
 467 match at mid frequencies from 400-1000 Hz between FSRR and SSRR and an overestimation of  
 468 sound absorption values above 1000 Hz for the small-scale reverberation room. This is attributed to  
 469 the use of Sabine's formulas instead of Eyring's as highlighted by Vercammen [21]. Moreover, it  
 470 should be highlighted that the differences obtained here between the small- and full-scale room or  
 471 impedance tube measurements are comparable with those obtained from absorption coefficient  
 472 measurements in 13 different laboratories Vercammen [21].



473

474 **Fig. 8.** Absorption coefficient of four materials in the conditions that minimized the normalized error:  
 475 samples with a size of  $60 \times 80 \text{ cm}^2$ , orientation 2, with sealed edges (Sample A, B, and D) and with  
 476 unsealed edges (Sample C). Also, the FSRR data report measurements with sealed edges and no  
 477 sealed edges, respectively. IT data are given after correction for diffuse incidence.

478

479

#### 480 4.3 Single number acoustic indices $\alpha_w$ , NRC, and SAA

481 Based on the above results, sound absorption indices  $\alpha_w$ , NRC, and SAA are derived from the IT,  
 482 FSRR and SSRR measurements. These single indices are useful for an immediate and practical  
 483 comparison of the performance of different materials. The higher the  $\alpha_w$ , SAA or the NRC values,  
 484 the better is the material capability in sound absorption. Their values normally range from 0 to 1, with  
 485 1 meaning 100% sound absorption for  $1 \text{ m}^2$  of material. These three indices have been compared in  
 486 former studies in order to estimate the differences and any possible drawback that could lead to flaws  
 487 in the performance comparison [45].

488 The weighted sound absorption coefficient  $\alpha_w$  is derived from practical sound absorption coefficients,  
 489  $\alpha_p$ . They are frequency-dependent values of the sound absorption coefficient, based on measurements

490 on one-third octave bands (according to EN ISO 354 [2]) and calculated in octave bands in accordance  
491 with EN ISO 11654 [46]. An averaged  $\alpha_p$  is calculated for the three one-third octave sound absorption  
492 coefficients within the octave. Weighted sound absorption coefficient  $\alpha_w$  can be obtained with the  
493 reference curve ( $\alpha_{250}=0.8$ ;  $\alpha_{500}=1$ ;  $\alpha_{1000}=1$ ;  $\alpha_{2000}=1$ ;  $\alpha_{4000}=0.9$ ). The curve is shifted in steps of 0.05  
494 towards the  $\alpha_p$  values until the sum of unfavourable deviations (this occurs when the measured value  
495 is lower than the value of the curve) is less or equal to 0.10. Finally, the weighted sound absorption  
496 coefficient is the value of the adjusted reference curve at 500 Hz.

497 The single number rating obtained from ASTM C423 [3] is the Sound Absorption Average (SAA).  
498 This is the average of the absorption coefficients for the twelve one-third octave bands from 200 Hz  
499 to 2500 Hz. The SAA supersedes the Noise Reduction Coefficient (NRC), which is the arithmetic  
500 average of the absorption coefficients determined at the octave bands of 250 Hz, 500 Hz, 1000 Hz  
501 and 2000 Hz, rounded to the nearest multiple of 0.05. The SAA value is rounded off the nearest 0.01  
502 increment. The ASTM standard does not introduce any shape indicators as the ISO method described  
503 above.

504 The expanded uncertainty, at a confidence level of 95% ( $k=2$ ), of the measured data under  
505 reproducibility conditions for  $\alpha_w$  has been evaluated according to Wittstock (2018) [41] and is equal  
506 to 0.07, i.e. twice the reproducibility standard deviation; the same value has been considered also for  
507 SAA and NRC, since no information is given on this regard in literature. As can be noticed in table  
508 2, there are a few differences among the single indices within each material data. The differences  
509 SSRR and FSRR related to  $\alpha_w$  are within a 0.10 for samples A and B, and 0.05 for samples C and D;  
510 differences related to NRC and SAA are within 0.05 for all the samples. Table 2 shows also the  
511 normalized error which has been evaluated for IT and SSRR measurements with respect to the FSRR  
512 data and SSRR with respect to the IT single values. The results can be considered compatible in most  
513 of the cases ( $E_n < 1$ ). However, it can be noticed that the differences between SSRR and FSRR are  
514 comparable to those between IT and FSRR.

515

516 Table 2: Comparison of results of single acoustic indices (NRC, SAA and  $\alpha_w$ ) for the four samples  
 517 (A, B, C, D) and three different test methods (IT, FSRR, and SSRR). Normalized error of the IT and  
 518 SSRR measurements with respect to the FSRR data and SSRR measurements with respect to IT data.  
 519  $E_n > 1$  are indicated in bold.

Sample	A			B			C			D		
Test Method	$\alpha_w$	SAA	NRC	$\alpha_w$	SAA	NRC	$\alpha_w$	SAA	NRC	$\alpha_w$	SAA	NRC
IT	0.70	0.73	0.75	0.75	0.77	0.75	0.20	0.32	0.30	0.65	0.67	0.65
FSRR	0.75	0.79	0.75	0.85	0.84	0.75	0.20	0.31	0.30	0.70	0.66	0.70
SSRR	0.65	0.78	0.80	0.75	0.87	0.85	0.15	0.26	0.25	0.70	0.68	0.70
$E_n$ (IT-FSRR)	0.51	0.61	0.00	<b>1.01</b>	0.71	0.00	0.00	0.10	0.00	0.51	0.10	0.51
$E_n$ (SSRR-FSRR)	<b>1.01</b>	0.10	0.51	<b>1.01</b>	0.30	<b>1.01</b>	0.51	0.51	0.51	0.00	0.20	0.00
$E_n$ (SSRR-IT)	0.51	0.51	0.51	0.00	<b>1.01</b>	<b>1.01</b>	0.51	0.61	0.51	0.51	0.10	0.51

520

521

#### 522 4.4 Comparison among the three methods

523 Finally, a summary of the advantages and disadvantages of the three methods are listed in Table 3. It  
 524 can be noticed that the SSRR presents a series of practical advantages that could allow for faster  
 525 measurements applying less resources, i.e. allows for an explorative phase in the early stages of the  
 526 design process as well as reduces the amount of material used for the production of the samples  
 527 leading to more sustainable ways of performing acoustic measurements. Moreover, these practical  
 528 features and faster feedback could ease the dissemination and increase awareness related to the  
 529 acoustic performance among designers and architects.

## 530 5 Conclusions

531 This work explored the range of application and reliability of the random-incidence absorption  
 532 coefficient measured within a small-scale reverberation room. Four different materials have been  
 533 measured with three different methods in the impedance tube (IT), full-scale (FSRR) and small-scale  
 534 (SSRR) reverberation room. It was shown that the SSRR presents several advantages compared to  
 535 the other methods, which have a practical relevance in the explorative design process of sound

536 absorptive building materials. After the research and development phase, the final material can be  
 537 sent to an independent acoustical laboratory for qualified ISO 354:2003 measurements.

538

539 Table 3: Synthetic comparison among IT, FSRR and SSRR methods.

Method	Sound incidence	Frequency range [Hz]	Sample area (m <sup>2</sup> )	Advantages	Disadvantages
IT	Normal	100-5000 (depending on the tube diameter)	< 0.1	<ul style="list-style-type: none"> <li>• reduced sample size</li> <li>• affordable measurement costs</li> <li>• limited wasted material</li> <li>• measurement time duration (&lt; 30 min)</li> </ul>	<ul style="list-style-type: none"> <li>• limited frequency range</li> <li>• normal sound incidence</li> <li>• 3D absorbing systems</li> </ul>
FSRR	Random	100-5000	10-12	<ul style="list-style-type: none"> <li>• sound incidence</li> <li>• limited edge effect</li> <li>• broad frequency range</li> <li>• 3D absorbing systems</li> </ul>	<ul style="list-style-type: none"> <li>• large sample size</li> <li>• huge measurement costs</li> <li>• high quantity of material to be dismantled</li> <li>• measurement time duration (&gt; 60 min)</li> </ul>
SSRR	Random	400-5000 (for porous materials) 1000-5000 (for thin rigid materials)	0.2-1.5	<ul style="list-style-type: none"> <li>• sound incidence</li> <li>• reduced sample size</li> <li>• affordable measurement costs</li> <li>• limited wasted material</li> <li>• measurement time duration (&lt;30 min)</li> <li>• 3D absorbing systems</li> </ul>	<ul style="list-style-type: none"> <li>• limited lower frequency range</li> <li>• edge effect</li> <li>• limited sample height</li> </ul>

540

541 The SSRR-based results have been compared against FSRR measurement, used as a reference, and  
 542 IT measurements. The analyses showed that normalized errors smaller than 1 – i.e. compatible results  
 543 – can be generally achieved, provided that some recommendations in measurement setup are needed.  
 544 First, to have reliable data a sample size close to 60×80 cm<sup>2</sup> is recommended; the size should be  
 545 placed with an oblique orientation on the room floor. Second, the sound absorption coefficients data  
 546 showed that the edge effect is more evident for thicker panels (>50cm) and smaller samples

547 (60x40cm<sup>2</sup>). For samples sizes of 60x80cm<sup>2</sup> the edge effect has been shown to be reduced also for  
548 thicker samples. This aspect should be investigated in a more systematic way including panels with  
549 thicknesses above those considered here in order to find a threshold of validity due to this parameter.  
550 Third, a sound absorption overestimation can take place depending on the sample thickness. Fourth,  
551 due to the limited diffusivity of the sound field, the SSRR method can be profitably adopted when  
552 the frequencies of interest lie above 400 Hz for porous materials and above 1000 Hz for thin low  
553 absorptive rigid materials. Nevertheless, as previously stated, since larger uncertainties in SSRRs and  
554 in FSRRs might occur especially for higher absorptive materials with ISO 354 method [41],  
555 compatibility ranges could be wider. Future research will be aimed at investigating this aspect.  
556 Within these use-cases, the discussed results show that that the small reverberation room is a reliable  
557 measurement tool in the frequency range 400-5000 Hz (for porous materials) and 1000-5000 Hz (for  
558 thin rigid materials), and therefore, can be considered as a valid alternative to the measurements in  
559 the full-scale or in the impedance tube. These might require a more systematic study that would  
560 consider also other variables (e.g. room volume variations) in order to define the proper range of  
561 application.  
562 Finally, this work has pointed out the advantages related to the possibility to test small-size samples,  
563 thus potentially leading to limited wasted material and transportation costs for the tested samples.  
564 Moreover, the sample arrangement in the SSRR set-up requires a shorter time, enabling in turn to  
565 dedicate an increased time to test different alternatives. Moreover, this could ease the dissemination  
566 and increase awareness related to the acoustic performance among designers and architects while  
567 pursuing more sustainable ways to perform acoustic measurements.

568

## 569 ACKNOWLEDGEMENTS

570 The authors are grateful to professors Arianna Astolfi, Marco Masoero and Alessandro Schiavi for  
571 the useful discussions and encouragement on this research. They would like to thank the architect

572 Chiara Devecchi, the engineers Paolo Onali and Davide Squarciapino for having provided some of  
573 the materials used in these measurements and Francesca Latorella and Andrea Gerbotto for their  
574 contribution to the small-scale measurements.

575 **References**

576

- 577 [1] ISO 10534-2:1998, Acoustics - Determination of sound absorption coefficient and impedance in  
578 impedance tubes - Part 2: Transfer-function method. International Organization for  
579 Standardization, Geneva, Switzerland.
- 580 [2] ISO 354:2003, Acoustics - measurement of sound absorption in a reverberation room. International  
581 Organization for Standardization, Geneva, Switzerland.
- 582 [3] ASTM C423-17:2017, Standard Test Method for Sound Absorption and Sound Absorption  
583 Coefficients by the Reverberation Room Method, ASTM International, West Conshohocken, PA.
- 584 [4] A. Alonso, F. Martellotta, Room acoustic modelling of textile materials hung freely in space: from  
585 the reverberation chamber to ancient churches, *Journal of Building Performance Simulation* 9  
586 (2016), 469-486. <http://dx.doi.org/10.1080/19401493.2015.1087594>
- 587 [5] J. R.Veen, J. Pan, P. Saha, Development of a Small Size Reverberation Room Standardized Test  
588 Procedure for Random Incidence Sound Absorption Testing, Proc. SAE conference 2005,  
589 Traverse City, USA, 2005.
- 590 [6] SAE j2883:2015 - Laboratory Measurement of Random Incidence Sound Absorption Tests Using  
591 a Small Reverberation Room. SAE International.
- 592 [7] P. Jackson, Design and Construction of a Small Reverberation Chamber, Proc. SAE conference  
593 2005, Traverse City, USA, 2005.
- 594 [8] G. Baldinelli, F. Bianchi, S. Endelis, A. Jakovics, G. L. Morini, S. Falcioni, S. Fantucci, V. Serra,  
595 M. A. Navacerrada, C. Díaz, A. Libbra, A. Muscio, F. Asdrubali, Thermal conductivity  
596 measurement of insulating innovative building materials by hot plate and heat flow meter devices:  
597 a round Robin test. *Int. J. Therm. Sci.* 139 (2019), 25-35.  
598 <https://doi.org/10.1016/j.ijthermalsci.2019.01.037>

- 599 [9] R. Del Rey, J. Alba, L. Bertó, A. Gregoriù, Small-sized reverberation chamber for the measurement  
600 of sound absorption, *Materiales de Construcción* 67 (2017), 139.  
601 <http://dx.doi.org/10.3989/mc.2017.07316>
- 602 [10] L. Pacheco Bastos, G. Da Silva Vieira de Melo, N. Sure Soeiro, Panels Manufactured from  
603 Vegetable Fibers: An Alternative Approach for Controlling Noises in Indoor Environments,  
604 *Advances in acoustic and vibration 2012*, (paper 698737). <http://dx.doi.org/10.1155/2012/698737>
- 605 [11] M. Kierzkowski, H. Law, J. Cotterill, Benefits of Reduced-size Reverberation Room Testing.  
606 *Proc. Acoustics 2017*, Perth, Australia, 2017.
- 607 [12] A. Rasa, Development of a small-scale reverberation room, *Proc. Acoustics 2016*, Brisbane,  
608 Australia, 2016.
- 609 [13] A. Chappuis, Small size devices for accurate acoustical measurements of materials and parts used  
610 in automobiles, *Proc. SAE conference 1993*; Traverse City, USA, 1993.
- 611 [14] A. De Bruijn, On the scattering of a plane wave by porous sound-absorbing strip, *Proc. Euronoise*  
612 2008, Paris, France, 2008.
- 613 [15] A. Duval, J.-F. Rondwau, L. Dejaeger, F. Sgard, N. Atalla, Diffuse field absorption coefficient  
614 simulation of porous materials in small reverberant chambers: finite size and diffusivity issues,  
615 *Proc. Congres Francais d'Acoustique 2010*, Lyon, France, 2010.
- 616 [16] A. Cops, J. Vanhaecht, K. Leppens, Sound Absorption in a Reverberation Room: Causes of  
617 Discrepancies on Measurement Results, *Appl. Acoust.* 46 (1995), 215-232.  
618 [https://doi.org/10.1016/0003-682X\(95\)00029-9](https://doi.org/10.1016/0003-682X(95)00029-9)
- 619 [17] M. Nolan, M. Vercammen, C. H. Jeong, Effects of different diffusers types on the diffusivity in  
620 reverberation chambers, *Proc. Euronoise 2018*, Crete, Greece, 2018.
- 621 [18] D. T. Bradley, M. Müller-Trapet, J. Adelgren, M. Vorländer, Effect of boundary diffusers in a  
622 reverberation chamber: Standardized diffuse field quantifiers. *J. Acoust. Soc. Am.* 135 (2014),  
623 1898-1906. <https://doi.org/10.1121/1.4866291>

- 624 [19] T.J. Cox, P. D'Antonio, *Acoustic Absorbers and Diffusers: Theory, Design and Application*, Spon  
625 Press, London, United Kingdom, 2004.
- 626 [20] C. Scrosati, F. Scamoni, M. Depalma, N. Granzotto, On the diffusion of the sound field in a  
627 reverberation room, Proc. 26th International Congress on Sound and Vibration, ICSV, Montréal,  
628 Canada, 2019.
- 629 [21] M. Vercammen, Improving the accuracy of sound absorption measurements according to ISO 354,  
630 Proc. ISRA 2010, Melbourne, Australia 2010.
- 631 [22] W. A. Davern, P. Dubout, First report on Australasian comparison measurements of sound  
632 absorption coefficients, Proc. CSIRIO 1980, Melbourne, 1980.
- 633 [23] N.B. Roozen, E.A. Piana, E. Deckers, C. Scrosati, On the numerical modelling of reverberant  
634 rooms, including a comparison with experiments, Proc. ICSV 2019, Montréal, Canada, 2019.
- 635 [24] M. Nolan, M. Vercammen, C. H. Jeong, J. Brunskog, The Use of a Reference Absorber for  
636 Absorption Measurements in a Reverberation Chamber, Proc. Forum Acusticum 2014, Krakow,  
637 Poland, 2014.
- 638 [25] C. Scrosati, D. Annesi, L. Barbaresi, R. Baruffa, F. D'Angelo, G. De Napoli, M. Depalma, A. Di  
639 Bella, S. Di Filippo, D. D'Orazio, M. Garai, N. Granzotto, V. Lori, F. Martellotta, A. Moschetto,  
640 F. Pompoli, A. Prato, P. Nataletti, F. Scamoni, A. Schiavi, F. Serpilli, Design Principles of the  
641 Italian Round Robin Test on Reverberation Rooms, Proc. of ICA 2019, Aachen, Germany, 2019.
- 642 [26] A. Prato, F. Casassa, A. Schiavi, Reverberation time measurements in non-diffuse acoustic field  
643 by the modal reverberation time, *Appl. Acoust.* 110 (2016), 160-169.  
644 <https://doi.org/10.1016/j.apacoust.2016.03.041>
- 645 [27] S. De Cesaris, D. D'Orazio, F. Morandi, M. Garai, Extraction of the envelope from impulse  
646 responses using pre-processed energy detection for early decay estimations, *J. Acoust. Soc. Am.*  
647 138 (2015), 2513-2523. <https://doi.org/10.1121/1.4931904>

- 648 [28] J. R. Veen, P. Saha, Feasibility of a standardized test procedure for random incidence sound  
649 absorption tests using a small size reverberation room, Proc. SAE conference 2003, Traverse City,  
650 USA, 2003.
- 651 [29] T. W. Bartel, Effect of absorber geometry on apparent absorption coefficients as measured in a  
652 reverberation chamber, *J. Acoust. Soc. Am.* 69 (1981), 1065-1074.  
653 <https://doi.org/10.1121/1.385685>
- 654 [30] F. Pompoli, P. Bonfiglio, K. V. Horoshenkov, A. Khan, L. Jaouen, F. Bécot, F. Sgard, F.  
655 Asdrubali, F. D'Alessandro, J. Hübel, N. Atalla, C. K. Amédin, W. Lauriks, L. Boeckx, How  
656 reproducible is the acoustical characterization of porous media?, *J. Acoust. Soc. Am.* 141 (2017),  
657 945-955. <https://doi.org/10.1121/1.4976087>
- 658 [31] D. Pilon, R. Panneton, F. Sgard, Behavioural criterion quantifying the effects of circumferential  
659 air gaps on porous materials in the standing wave tube, *J. Acoust. Soc. Am.* 116 (2004), 344-356.  
660 <https://doi.org/10.1121/1.1756611>
- 661 [32] R. Spagnolo, G. Benedetto, Reverberation time in enclosures: The surface reflection law and the  
662 dependence of the absorption coefficient on the angle of incidence, *J. Acoust. Soc. Am.* 77 (1985),  
663 1447-1451. <https://doi.org/10.1121/1.392039>
- 664 [33] ISO 9613:1993, Acoustics – attenuation of sound during propagation outdoors – Part 1: calculation  
665 of the absorption of sound by the atmosphere. International Organization for Standardization,  
666 Geneva, Switzerland.
- 667 [34] ISO 17497-1:2004, Acoustics – sound-scattering properties of surfaces – Part 1: measurement of  
668 the random-incidence scattering coefficient in a reverberation room. International Organization  
669 for Standardization, Geneva, Switzerland.
- 670 [35] L. Shtrepi, A. Astolfi, G. D'Antonio, G. Vannelli, G. Barbato, S. Mauro, A. Prato, Accuracy of  
671 the random-incidence scattering coefficient measurement. *Appl. Acoust.* 106 (2016), 23-35.  
672 <https://doi.org/10.1016/j.apacoust.2015.12.021>

- 673 [36] C. -H. Jeong, Diffuse Sound Field: Challenges and Misconceptions. Proc. INTER-NOISE 2016,  
674 Hamburg, Germany.
- 675 [37] A. Gerbotto, Caratterizzazione di una camera riverberante in scala - Acoustic characterization of  
676 a scaled reverberation room, Master Thesis, Politecnico di Torino, 2016.
- 677 [38] ITA-Toolbox for MATLAB® Developed at the Institute of Technical Acoustics at RWTH Aachen  
678 University.
- 679 [39] ISO/IEC 17043:2010, Conformity assessment - General requirements for proficiency testing.  
680 International Organization for Standardization, Geneva, Switzerland.
- 681 [40] JCGM 100 2008 Evaluation of Measurement Data — Guide to the Expression of Uncertainty in  
682 Measurement (*GUM*), Joint Committee for Guides in Metrology, Sèvres, France.
- 683 [41] V. Wittstock, Determination of Measurement Uncertainties in Building Acoustics by  
684 Interlaboratory Tests. Part 2: Sound Absorption Measured in Reverberation Rooms, *Acta Acust.*  
685 United with *Acust.* 104 (2018), 999 – 1008. <https://doi.org/10.3813/AAA.919266>
- 686 [42] D. George, P. Mallery, SPSS for Windows Step by Step: A Simple Guide and Reference 17.0  
687 Update. 10th Edition, Pearson, Boston, 2010.
- 688 [43] A. Schiavi and A. Prato, Valuation of sound absorption: an experimental comparative study among  
689 reverberation room, impedance tube and airflow resistivity-based models, Proc. ICSV 2019,  
690 Montréal, Canada, 2019.
- 691 [44] Jain, S., Joshi, M., Bankar, H., Kamble, P., Yadav P., Karanth N. Measurement and Prediction of  
692 Sound Absorption of Sound Package Materials in Large and Small Reverberation Chambers, Proc  
693 SAE conference 2017, Traverse City, USA, 2017.
- 694 [45] J. Białek, E. Nowicka, Comparison of sound absorption ratings calculated according to ISO and  
695 ASTM standards, Proc. OSA 2016, Warsaw, Poland, 2016.
- 696 [46] ISO 11654:1997, Acoustics - Sound absorbers for use in buildings - Rating of sound absorption.  
697 International Organization for Standardization, Geneva, Switzerland.

Appendix A

Sound absorption coefficient ( $\alpha_s$ ) and related uncertainty ( $U$ ) for material A measured in SSRR, IT and FSRR. Given the background noise criterion (section 2.4), the SSRR data are valid for 250-5000 Hz. IT<sub>n</sub> shows the data for normal-incidence sound absorption coefficients.

SSRR		Frequency [Hz]																		
Size [cm <sup>2</sup> ]	Orientation		100	125	160	200	250	315	400	500	630	800	1000	1250	1600	2000	2500	3150	4000	5000
60x40	O1	$\alpha_s$	0.11	0.24	0.00	0.42	0.61	0.53	0.52	0.64	0.68	1.10	1.29	1.10	1.10	1.05	1.13	1.23	1.14	1.04
		$U$	0.17	0.23	0.06	0.24	0.28	0.22	0.18	0.19	0.18	0.24	0.27	0.24	0.24	0.23	0.23	0.24	0.28	0.30
	O2	$\alpha_s$	0.10	0.20	0.00	0.40	0.60	0.48	0.53	0.60	0.68	1.03	1.15	1.20	1.20	0.96	1.21	1.10	1.17	0.94
		$U$	0.15	0.20	0.06	0.24	0.28	0.21	0.19	0.18	0.18	0.23	0.24	0.26	0.25	0.22	0.25	0.26	0.30	0.34
	O3	$\alpha_s$	0.09	0.17	0.00	0.36	0.58	0.49	0.58	0.56	0.63	1.02	1.05	1.22	1.27	0.90	1.22	1.18	1.15	1.02
		$U$	0.15	0.18	0.06	0.22	0.27	0.21	0.20	0.17	0.17	0.22	0.23	0.26	0.26	0.21	0.25	0.27	0.30	0.35
60x60	O1	$\alpha_s$	0.00	0.00	0.01	0.32	0.46	0.51	0.56	0.59	0.70	1.17	0.98	1.04	1.04	0.83	1.00	0.95	0.94	0.85
		$U$	0.06	0.06	0.06	0.20	0.23	0.21	0.19	0.18	0.19	0.25	0.22	0.23	0.23	0.20	0.22	0.24	0.27	0.33
	O2	$\alpha_s$	0.00	0.00	0.04	0.33	0.47	0.47	0.58	0.63	0.80	1.06	1.00	1.06	0.96	0.86	1.00	0.92	1.07	0.91
		$U$	0.06	0.06	0.08	0.21	0.23	0.20	0.20	0.19	0.20	0.23	0.22	0.23	0.21	0.20	0.22	0.24	0.29	0.33
60x80	O1	$\alpha_s$	0.00	0.00	0.18	0.26	0.38	0.49	0.57	0.72	0.96	1.04	1.08	1.02	1.09	0.92	0.96	0.95	0.97	0.85
		$U$	0.06	0.06	0.16	0.18	0.20	0.21	0.20	0.20	0.23	0.23	0.23	0.23	0.23	0.21	0.22	0.24	0.28	0.33
	O2	$\alpha_s$	0.00	0.00	0.14	0.29	0.33	0.43	0.61	0.74	0.97	1.05	1.07	0.94	1.02	0.98	0.98	0.96	0.98	0.87
		$U$	0.06	0.06	0.14	0.19	0.18	0.19	0.21	0.21	0.23	0.23	0.23	0.21	0.22	0.22	0.22	0.24	0.28	0.33
	O3	$\alpha_s$	0.00	0.01	0.14	0.24	0.32	0.49	0.56	0.73	0.85	1.07	1.03	0.94	1.05	0.88	0.95	0.92	0.98	0.88
		$U$	0.06	0.07	0.14	0.16	0.18	0.21	0.19	0.21	0.21	0.23	0.23	0.21	0.23	0.21	0.22	0.24	0.28	0.33
IT	$\alpha$	0.20	0.21	0.24	0.30	0.40	0.53	0.64	0.76	0.84	0.88	0.89	0.89	0.88	0.86	0.84	0.82	0.83	0.79	
	$U$	0.01	0.02	0.03	0.04	0.04	0.03	0.03	0.04	0.05	0.04	0.03	0.03	0.02	0.03	0.04	0.04	0.03	0.02	
IT <sub>n</sub>	$\alpha_0$	0.14	0.15	0.17	0.22	0.30	0.42	0.53	0.66	0.76	0.81	0.83	0.82	0.80	0.78	0.75	0.73	0.74	0.69	
	$U$	0.01	0.02	0.03	0.04	0.04	0.03	0.03	0.04	0.05	0.04	0.03	0.03	0.02	0.03	0.04	0.04	0.03	0.02	
FSRR	$\alpha_s$	0.09	0.13	0.23	0.32	0.52	0.64	0.79	0.81	0.92	0.94	0.96	0.93	0.95	0.91	0.86	0.84	0.83	0.79	
	$U$	0.07	0.08	0.09	0.10	0.12	0.13	0.12	0.11	0.11	0.11	0.11	0.11	0.11	0.11	0.10	0.11	0.13	0.16	

Appendix B

Sound absorption coefficient ( $\alpha_s$ ) and related uncertainty ( $U$ ) for material B measured in SSRR, IT and FSRR. Given the background noise criterion (section 2.4), the SSRR data are valid for 250-5000 Hz. IT<sub>n</sub> shows the data for normal-incidence sound absorption coefficients.

SSRR			Frequency [Hz]																	
Size [cm <sup>2</sup> ]	Orientation		100	125	160	200	250	315	400	500	630	800	1000	1250	1600	2000	2500	3150	4000	5000
60x40	O1	$\alpha_s$	0.11	0.24	0.00	0.42	0.61	0.53	0.52	0.64	0.68	1.10	1.29	1.10	1.10	1.05	1.13	1.23	1.14	1.04
		$U$	0.17	0.23	0.06	0.24	0.28	0.22	0.18	0.19	0.18	0.24	0.27	0.24	0.23	0.23	0.24	0.28	0.30	0.35
	O2	$\alpha_s$	0.10	0.20	0.00	0.40	0.60	0.48	0.53	0.60	0.68	1.03	1.15	1.20	1.20	0.96	1.21	1.10	1.17	0.94
		$U$	0.15	0.20	0.06	0.24	0.28	0.21	0.19	0.18	0.18	0.23	0.24	0.26	0.25	0.22	0.25	0.26	0.30	0.34
	O3	$\alpha_s$	0.09	0.17	0.00	0.36	0.58	0.49	0.58	0.56	0.63	1.02	1.05	1.22	1.27	0.90	1.22	1.18	1.15	1.02
		$U$	0.15	0.18	0.06	0.22	0.27	0.21	0.20	0.17	0.17	0.22	0.23	0.26	0.26	0.21	0.25	0.27	0.30	0.35
60x60	O1	$\alpha_s$	0.00	0.00	0.01	0.32	0.46	0.51	0.56	0.59	0.70	1.17	0.98	1.04	1.04	0.83	1.00	0.95	0.94	0.85
		$U$	0.06	0.06	0.06	0.20	0.23	0.21	0.19	0.18	0.19	0.25	0.22	0.23	0.23	0.20	0.22	0.24	0.27	0.33
	O2	$\alpha_s$	0.00	-0.09	0.04	0.33	0.47	0.47	0.58	0.63	0.80	1.06	1.00	1.06	0.96	0.86	1.00	0.92	1.07	0.91
		$U$	0.06	-0.01	0.08	0.21	0.23	0.20	0.20	0.19	0.20	0.23	0.22	0.23	0.21	0.20	0.22	0.24	0.29	0.33
60x80	O1	$\alpha_s$	0.00	0.00	0.18	0.26	0.38	0.49	0.57	0.72	0.96	1.04	1.08	1.02	1.09	0.92	0.96	0.95	0.97	0.85
		$U$	0.06	0.06	0.16	0.18	0.20	0.21	0.20	0.20	0.23	0.23	0.23	0.23	0.23	0.21	0.22	0.24	0.28	0.33
	O2	$\alpha_s$	0.00	0.00	0.14	0.29	0.33	0.43	0.61	0.74	0.97	1.05	1.07	0.94	1.02	0.98	0.98	0.96	0.98	0.87
		$U$	0.06	0.06	0.14	0.19	0.18	0.19	0.21	0.21	0.23	0.23	0.23	0.21	0.22	0.22	0.22	0.24	0.28	0.33
	O3	$\alpha_s$	0.00	0.01	0.14	0.24	0.32	0.49	0.56	0.73	0.85	1.07	1.03	0.94	1.05	0.88	0.95	0.92	0.98	0.88
		$U$	0.06	0.07	0.14	0.16	0.18	0.21	0.19	0.21	0.21	0.23	0.23	0.21	0.23	0.21	0.22	0.24	0.28	0.33
IT		$\alpha$	0.10	0.15	0.23	0.35	0.49	0.63	0.74	0.84	0.88	0.90	0.90	0.89	0.88	0.88	0.87	0.85	0.86	0.83
		$U$	0.04	0.04	0.02	0.00	0.01	0.01	0.01	0.01	0.01	0.01	0.01	0.01	0.01	0.01	0.01	0.01	0.01	0.02
IT <sub>n</sub>		$\alpha_0$	0.07	0.10	0.17	0.26	0.38	0.52	0.64	0.75	0.81	0.83	0.83	0.82	0.81	0.81	0.79	0.77	0.79	0.74
		$U$	0.04	0.04	0.02	0.00	0.01	0.01	0.01	0.01	0.01	0.01	0.01	0.01	0.01	0.01	0.01	0.01	0.01	0.02
FSRR		$\alpha_s$	0.09	0.18	0.28	0.52	0.65	0.75	0.82	0.86	0.91	0.90	0.99	0.96	0.95	0.90	0.90	0.87	0.85	0.80
		$U$	0.07	0.09	0.11	0.14	0.15	0.14	0.13	0.12	0.11	0.10	0.11	0.11	0.11	0.10	0.11	0.12	0.13	0.16

### Appendix C

Sound absorption coefficient ( $\alpha_s$ ) and related uncertainty ( $U$ ) for material C measured in SSRR, IT and FSRR. Given the background noise criterion (section 2.4), the SSRR data are valid for 250-5000 Hz. IT<sub>n</sub> shows the data for normal-incidence sound absorption coefficients.

SSRR		Frequency [Hz]																		
Size [cm <sup>2</sup> ]	Orientation		100	125	160	200	250	315	400	500	630	800	1000	1250	1600	2000	2500	3150	4000	5000
60x40	O1	$\alpha_s$	0.00	0.00	0.00	0.01	0.03	0.02	0.02	0.07	0.10	0.12	0.32	0.38	1.12	1.12	1.12	1.07	1.21	0.98
		$U$	0.06	0.06	0.06	0.07	0.07	0.07	0.07	0.07	0.07	0.08	0.08	0.11	0.12	1.07	1.07	1.07	0.26	0.31
	O2	$\alpha_s$	0.00	0.00	0.00	0.08	0.06	0.03	0.02	0.06	0.10	0.14	0.28	0.43	1.21	1.21	1.21	1.02	1.22	0.97
		$U$	0.06	0.06	0.06	0.09	0.08	0.07	0.06	0.07	0.08	0.08	0.11	0.13	1.18	1.18	1.18	0.25	0.31	0.34
	O3	$\alpha_s$	0.00	0.00	0.00	0.09	0.07	0.03	0.04	0.08	0.11	0.09	0.30	0.51	1.32	1.32	1.32	1.03	1.15	0.97
		$U$	0.06	0.06	0.06	0.10	0.09	0.07	0.07	0.08	0.08	0.07	0.11	0.14	1.28	1.28	1.28	0.25	0.30	0.34
60x60	O1	$\alpha_s$	0.02	0.05	0.05	0.03	0.10	0.04	0.03	0.08	0.11	0.14	0.34	0.46	0.50	0.54	0.82	0.93	1.02	1.02
		$U$	0.08	0.10	0.09	0.07	0.10	0.07	0.07	0.08	0.08	0.08	0.11	0.14	0.15	0.16	0.20	0.24	0.28	0.35
	O2	$\alpha_s$	0.04	0.04	0.08	0.01	0.09	0.04	0.03	0.07	0.12	0.14	0.37	0.36	0.44	0.55	0.79	0.96	1.14	1.03
		$U$	0.10	0.09	0.10	0.06	0.09	0.07	0.07	0.07	0.08	0.08	0.12	0.12	0.14	0.16	0.20	0.24	0.30	0.35
60x80	O1	$\alpha_s$	0.00	0.00	0.05	0.00	0.02	0.02	0.03	0.06	0.12	0.15	0.30	0.40	0.50	0.57	0.90	1.01	1.12	1.00
		$U$	0.06	0.06	0.09	0.06	0.07	0.06	0.07	0.07	0.08	0.08	0.11	0.13	0.15	0.16	0.21	0.25	0.29	0.34
	O2	$\alpha_s$	0.00	0.00	0.00	0.00	0.02	0.03	0.06	0.05	0.12	0.12	0.33	0.43	0.52	0.58	0.87	1.02	1.12	1.08
		$U$	0.06	0.06	0.06	0.06	0.07	0.07	0.07	0.07	0.08	0.08	0.11	0.13	0.15	0.16	0.21	0.25	0.29	0.35
	O3	$\alpha_s$	0.00	0.00	0.04	0.00	0.04	0.03	0.05	0.05	0.13	0.15	0.32	0.43	0.44	0.59	0.85	0.90	1.00	1.00
		$U$	0.06	0.06	0.08	0.06	0.08	0.07	0.07	0.07	0.08	0.08	0.11	0.13	0.14	0.17	0.21	0.24	0.28	0.34
IT	$\alpha$	0.27	0.16	0.17	0.13	0.14	0.13	0.12	0.10	0.19	0.24	0.33	0.45	0.56	0.67	0.79	0.91	0.95	0.91	
	$U$	0.03	0.02	0.02	0.01	0.01	0.00	0.00	0.00	0.00	0.01	0.02	0.04	0.08	0.10	0.07	0.05	0.01	0.04	
IT <sub>n</sub>	$\alpha_0$	0.20	0.11	0.12	0.09	0.09	0.09	0.08	0.07	0.14	0.18	0.25	0.35	0.45	0.56	0.70	0.85	0.92	0.86	
	$U$	0.03	0.02	0.02	0.01	0.01	0.00	0.00	0.00	0.00	0.01	0.02	0.04	0.08	0.10	0.07	0.05	0.01	0.04	
FSRR	$\alpha_s$	0.02	0.02	0.02	0.05	0.06	0.09	0.11	0.14	0.23	0.30	0.34	0.45	0.54	0.66	0.74	0.83	0.85	0.89	
	$U$	0.04	0.04	0.03	0.04	0.04	0.04	0.04	0.04	0.04	0.05	0.05	0.06	0.07	0.08	0.09	0.10	0.11	0.13	0.17

Appendix D

Sound absorption coefficient ( $\alpha_s$ ) and related uncertainty ( $U$ ) for material D measured in SSRR, IT and FSRR. Given the background noise criterion (section 2.4), the SSRR data are valid for 250-5000 Hz. IT<sub>n</sub> shows the data for normal-incidence sound absorption coefficients.

SSRR		Frequency [Hz]																		
Size [cm <sup>2</sup> ]	Orientation		100	125	160	200	250	315	400	500	630	800	1000	1250	1600	2000	2500	3150	4000	5000
60x40	O1	$\alpha_s$	0.07	0.28	0.39	0.65	0.78	0.98	1.07	0.74	1.00	1.21	1.36	0.90	0.85	0.95	1.00	1.21	1.20	1.01
		$U$	0.12	0.26	0.28	0.35	0.34	0.35	0.32	0.21	0.24	0.25	0.28	0.21	0.20	0.22	0.22	0.22	0.27	0.30
	O2	$\alpha_s$	0.03	0.26	0.38	0.72	0.79	0.93	0.85	0.70	0.94	1.11	1.29	0.88	1.03	0.90	1.05	1.13	1.25	1.10
		$U$	0.09	0.25	0.27	0.38	0.34	0.34	0.26	0.20	0.23	0.24	0.27	0.20	0.22	0.21	0.23	0.26	0.31	0.35
	O3	$\alpha_s$	0.00	0.26	0.40	0.70	0.88	0.92	0.90	0.72	0.94	1.19	1.13	0.99	1.02	0.87	0.99	1.04	1.28	0.96
		$U$	0.06	0.25	0.29	0.37	0.38	0.34	0.28	0.20	0.23	0.25	0.24	0.22	0.22	0.21	0.22	0.25	0.31	0.34
60x60	O1	$\alpha_s$	0.09	0.37	0.35	0.53	0.68	0.67	0.58	0.67	0.75	0.93	0.91	0.84	0.78	0.98	0.96	0.98	1.26	1.07
		$U$	0.14	0.33	0.26	0.29	0.30	0.26	0.20	0.19	0.20	0.21	0.21	0.20	0.19	0.22	0.22	0.25	0.31	0.35
	O2	$\alpha_s$	0.20	0.41	0.37	0.54	0.59	0.67	0.64	0.61	0.76	1.04	0.84	0.87	1.02	0.87	0.97	1.05	1.25	1.09
		$U$	0.25	0.35	0.27	0.30	0.27	0.26	0.21	0.18	0.20	0.23	0.19	0.20	0.22	0.21	0.22	0.25	0.31	0.35
60x80	O1	$\alpha_s$	0.15	0.24	0.34	0.33	0.47	0.66	0.53	0.69	0.70	0.69	0.73	0.71	0.72	0.76	0.80	1.05	1.12	0.99
		$U$	0.21	0.23	0.25	0.21	0.23	0.26	0.19	0.20	0.19	0.17	0.18	0.18	0.18	0.19	0.20	0.25	0.29	0.34
	O2	$\alpha_s$	0.24	0.25	0.33	0.40	0.60	0.66	0.53	0.61	0.67	0.74	0.69	0.84	0.80	0.85	0.83	0.99	1.19	0.98
		$U$	0.29	0.24	0.24	0.24	0.28	0.26	0.19	0.18	0.18	0.18	0.17	0.20	0.19	0.20	0.20	0.25	0.30	0.34
	O3	$\alpha_s$	0.14	0.26	0.38	0.43	0.54	0.65	0.66	0.78	0.68	0.70	0.73	0.59	0.76	0.85	0.86	0.98	1.11	0.92
		$U$	0.19	0.25	0.27	0.25	0.25	0.26	0.22	0.22	0.18	0.17	0.18	0.16	0.18	0.20	0.21	0.25	0.29	0.34
IT	$\alpha$	0.38	0.42	0.55	0.64	0.71	0.74	0.75	0.74	0.72	0.68	0.64	0.61	0.58	0.58	0.61	0.65	0.75	0.84	
	$U$	0.06	0.02	0.04	0.06	0.08	0.08	0.07	0.07	0.06	0.06	0.05	0.04	0.03	0.02	0.02	0.01	0.04	0.04	
IT <sub>n</sub>	$\alpha_0$	0.29	0.32	0.44	0.53	0.60	0.64	0.65	0.63	0.62	0.57	0.53	0.50	0.47	0.47	0.50	0.54	0.65	0.75	
	$U$	0.06	0.02	0.04	0.06	0.08	0.08	0.07	0.07	0.06	0.06	0.05	0.04	0.03	0.02	0.02	0.01	0.04	0.04	
FSRR	$\alpha_s$	0.43	0.50	0.53	0.54	0.58	0.68	0.66	0.70	0.72	0.69	0.65	0.64	0.67	0.71	0.73	0.78	0.86	0.85	
	$U$	0.24	0.21	0.18	0.15	0.13	0.13	0.11	0.10	0.09	0.09	0.08	0.08	0.09	0.09	0.10	0.11	0.13	0.16	